International Journal of Adhesion & Adhesives 57 (2015) 49–56

Contents lists available at ScienceDirect

International Journal of Adhesion & Adhesives

journal homepage: www.elsevier.com/locate/ijadhadh

Effects of primer and annealing treatments on the shear strength between anodized Ti6Al4V and epoxy

Peigang He, Mingyue Huang, Stefan Fisher, Chee Yoon Yue, Jinglei Yang *

School of Mechanical & Aerospace Engineering, Nanyang Technological University, 50 Nanyang Avenue, Singapore 639798, Singapore

ARTICLE INFO

Article history:
Accepted 10 October 2014
Available online 23 October 2014

Keywords:
A. Hybrid
B. Fracture
B. Interface/interphase
D. Fractography

ABSTRACT

The effects of primer and annealing treatments on the shear strength between anodized Ti6Al4V and epoxy were investigated. Primer coating improved the shear strength between anodized Ti alloy and epoxy by up to 81.3% using concurrent curing compared with that of control specimens. After annealing of anodized Ti alloy and applying primer, the shear strength of the specimen was further increased by 6.4% due to the formation of stable TiO_2 transferred from TiO in the anodization process. SEM analysis revealed the specimen without primer and annealing treatments showed adhesive failure between epoxy–alloy interface and discontinuous cohesive failure of epoxy. Primer coating initiated a new interfacial failure mode between the oxide layer and alloy due to the improved bonding strength between epoxy and oxide layer. In addition, annealing and primer treatments generated large tracts of epoxy continuous cohesive failure, showing good agreement with its higher shear strength and work of fracture.

1. Introduction

Ti6Al4V is currently widely used for marine components, steam turbine blades, structural forgings, and fasteners, due to its desirable properties such as high fatigue strength, machinability, weldability, and corrosion resistance [1]. One of the most important applications are titanium-based fiber-metal laminates (FML), which have advantages of combined benefits from Ti alloy and fiber reinforced plastic (FRP) composites [2–5], including durability and fire resistance, reliable anti-permeability, high specific strength and stiffness, diverse failure modes, among others. Thus this kind of composite has drawn substantial attention from the offshore industry, for example deepwater risers being an alternative to the existing steel catenary risers in our project. However, to achieve the above desired properties, Ti–FRP interface property plays the critical role in determining the overall performance of the hybrid Titanium-based fiber-metal laminates. Especially for deepwater operation, interface between Ti and FRP is more susceptible to the harsh chemical and mechanical marine environments, which is one of the biggest concerns on this kind of composite. Until now, many kinds of mechanical, chemical, electrochemical and energetic surface treatments have been developed, such as abrasion and grit blasting [6–8], etching [9–12], coupling agent [13,14], plasma-spray and laser treatment [15–17], sol/gel methods [18,19], anodization [20–27], microarc oxidation [28,29], laser shock peening [30], among others, to produce a strong and durable adhesive joint between Ti alloy and composites.

In our recent research we reported that anodization of Ti6Al4V in sodium hydroxide based electrolyte at 40 °C was an efficient method to enhance shear strength and work of fracture between Ti6Al4V and epoxy [31]. And both parameters were increased by 317.2% and 533.6%, respectively, compared to those of untreated specimen. However, interface failure between anodized Ti6Al4V and epoxy was observed which indicated the bonding strength can still be optimized. Primer might be a possible solution [32–37]. Works done by Rider et al. [38] proved that addition of primer was an efficient methods to improve toughness and durability of bonded aluminum joints. And Brack et al. [39] reported that the addition of a thin primer film to the titanium slowed degradation rates and led to higher fracture toughness at longer humid-exposure times.

In this paper, aiming to further enhance the interface properties, primer together with annealing treatments of the anodized Ti6Al4V was applied and their effects on the mechanical properties and multiple cohesive and adhesive failure behaviors were investigated. This provides a scalable approach and direct reference for designing and manufacturing our Ti–FRP hybrid composite structure for marine and offshore applications.

* Corresponding author. Tel.: +65 6790 6906; fax: +65 6792 4062.
E-mail address: MJLYang@ntu.edu.sg (J. Yang).

http://dx.doi.org/10.1016/j.ijadhadh.2014.10.004
0143-7496/

2. Material and experimental procedure

2.1. Materials

The metal adherends used in the experiment are Ti6Al4V alloy (Grade 5) which was composed of α-Ti and β-Ti. They were ground with sandpapers of P800, P1200, P2400, P4000 and SiO_2 polishing paste consecutively, ultrasonically washed with distilled water and acetone, finally dried for anodization. The anodization was carried out in sodium based electrolyte at 40 °C for 15 min. The electrolyte was prepared from the solution of NaOH (7.5 M), $Na_2C_4H_4O_6 \cdot 2H_2O$ (0.2 M) and EDTA (0.1 M). A DC power unit was employed to generate voltage of 15 V. A water bath was used to keep the anodizing temperature to be 40 °C. The Ti plate was used as the anode and a thin stainless steel foil was used as the counter electrode.

The preparation of single-lap-joint specimens are the same as described in literature [31]. After anodization, thermal annealing treatment on one batch of Ti6Al4V specimens was performed at 500 °C in air for 5 h. Table 1 shows the mechanical properties of Ti6Al4V before and after annealing at 500 °C for 5 h. After annealing, there are slightly increases in yield strength, ultimate strength and modulus.

Bisphenol-F epoxy resin (DER 354, Dow Chemical) was used as polymer adhesive, hardened by amine based curing agent (EPOLAM 5015, Axson). Epoxy resin was mixed with hardener for 5 min and then degassed for 15 min in a vacuum oven before application to the Ti surface.

The primer used in this investigation was BR-127 (Cytec Industries Inc.), a kind of epoxy/phenolic resin diluted in 2-butanone and 2-ethoxyethanol. The primer film was prepared on the Ti6Al4V alloy surface by spin-coating technology with a rotational speed of 400 rpm. The thickness of the primer coating was 3–5 μm, which was measured by Coating Thickness Gages (PosiTector 6000).

Epoxy resin was carefully spread on the specimens without introducing air bubbles. Align the test specimens such that the overlap is 25 ± 0.25 mm. After cleaning away the excess epoxy resin, the specimens were cured at 35 °C for 24 h, 50 °C for 24 h, and 120 °C for 30 min in the oven. The thickness of the epoxy layer in the cured specimen is 0.4 mm. During the preparation process, no pressure was applied when forming the joints.

The Ti6Al4V-epoxy without primer were denoted as S-WP; the one with primer cured at 120 °C for 30 min before and after the application of epoxy, were denoted as S-P; and the one with primer and cured at 120 °C for 30 min after the application of epoxy, were denoted as S-P120.

2.2. Surface characterization

The morphologies of the specimens coated with gold were examined by field emission gun scanning electron microscopy (FEG-SEM, JEOL JSM7600F) equipped with an EDX detector, operated at 20 kV for EDX analysis and backscattered electron imaging. An X-ray photoelectron spectroscopy (XPS, Axis-ultra, Kratos) was used to detect the chemical composition of the oxide layers. In the XPS experiment, an Al *Kα* X-ray source was used at 15 kV and 10 mA. The measured binding energies were calibrated by the C 1s (hydrocarbon C–C, C–H) of 285 eV.

Table 1
Mechanical properties of Ti6Al4V (Grade 5) before and after annealing at 500 °C for 5 h.

Ti6Al4V	Yield strength (MPa)	Ultimate Strength (MPa)	Modulus of elasticity (GPa)
Before annealing	910 ± 38	1000 ± 46	114 ± 11
After annealing	928 ± 42	1020 ± 52	116 ± 9

2.3. Apparent shear strength

Apparent shear strengths were measured using a universal testing machine (Instron 5569) according to ASTM D1002 with the modified specimen size of 14 mm × 100 mm × 2 mm. Different joint areas were used, i.e., 14 mm × 25 mm in section of effects of primer (Section 3.1) and 14 mm × 14 mm in section of effects of annealing treatment (Section 3.2). Specimen geometries are shown in Fig. 1. The testing speed was 1.3 mm/min. Load–displacement curves were recorded for further analysis. Work of fracture was calculated by the area in the load–displacement curves. Six specimens were used for each testing condition and average values with standard deviations were finally reported.

3. Results and discussion

3.1. Effects of primer on the shear strength between Ti6Al4V and epoxy

Fig. 2 shows the SEM and selected-area EDX results of the anodized Ti6Al4V with primer coating. Fig. 1(b)–(d) indicates the elemental distribution in the selected area in (a), and they correspond to the EDX results of Ti, Al and C via area scanning. According to the EDX results, In the SEM image the gray domains correspond to the Ti6Al4V substrate, while the dark ones correspond to the primer. Thus the Ti alloy was discontinuously covered by the primer coating.

Fig. 3 presents shear strength and load–displacement between Ti6Al4V-epoxy before and after the application of primer. For both polished Ti6Al4V and anodized Ti6Al4V, after the application of primer coating, shear strength was improved significantly. Meanwhile, optimized curing strategy can further increase the shear strength. Taking the anodized Ti6Al4V-epoxy for example, shear strength of S-WP was only 8.01 ± 1.09 MPa. After the application of primer, shear strength of 12.14 ± 1.2 MPa was obtained, which was notably improved by 51.6% with respect to that of S-WP. A distinct maximum of 14.52 ± 0.86 MPa was achieved for the specimen S-P120 using optimized curing strategy, which was higher than that of S-P by 19.6% and higher than that of S-WP by 81.3%. Typical load–displacement curves also showed that maximum load was achieved for sample using primer and optimized curing strategy (S-P120). Meanwhile, S-P120 also exhibited much higher work of fracture than S-WP by comparing their respective areas in the load–displacement curve. The shear strength of Ti-epoxy in this investigation was much lower than ~37 MPa, which was reported by Palmieri et al. [40]. This might be due to different mechanical properties of the resin (PETI of high toughness vs. brittle EPOLAM 5015) and failure modes of the system as discussed below.

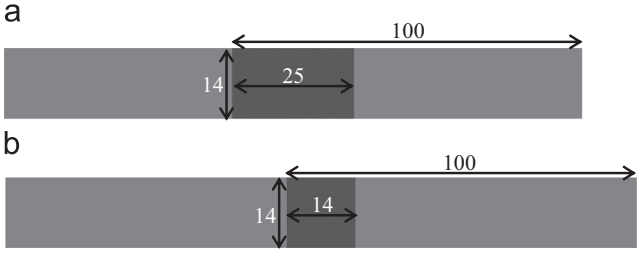

Fig. 1. Ti-epoxy specimen geometries (the black areas refer to the joints) (unit: mm).

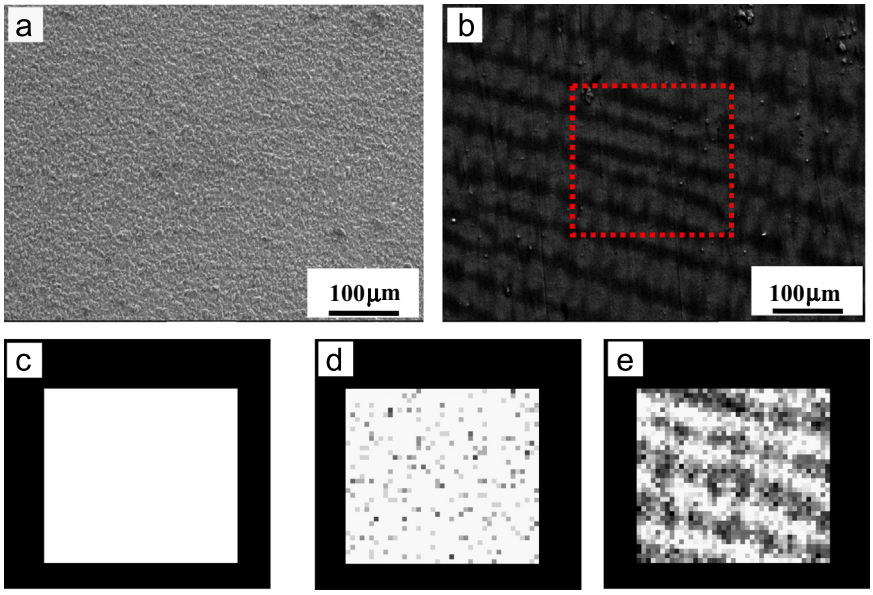

Fig. 2. SEM images of anodized Ti before (a) and after primer coating (b), and selected-area EDX results of Ti (c), Al (d) and C (e) of the squared area in (b).

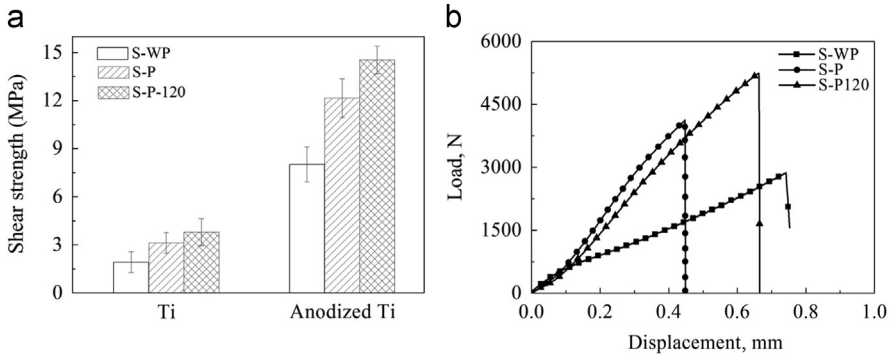

Fig. 3. Mechanical properties of Ti-epoxy joints: (a) shear strength (Ti columns refer to joints using polished Ti adherends, and anodized Ti columns refer to joints using anodized Ti adherends); (b) typical load–displacement curves of joints using anodized Ti.

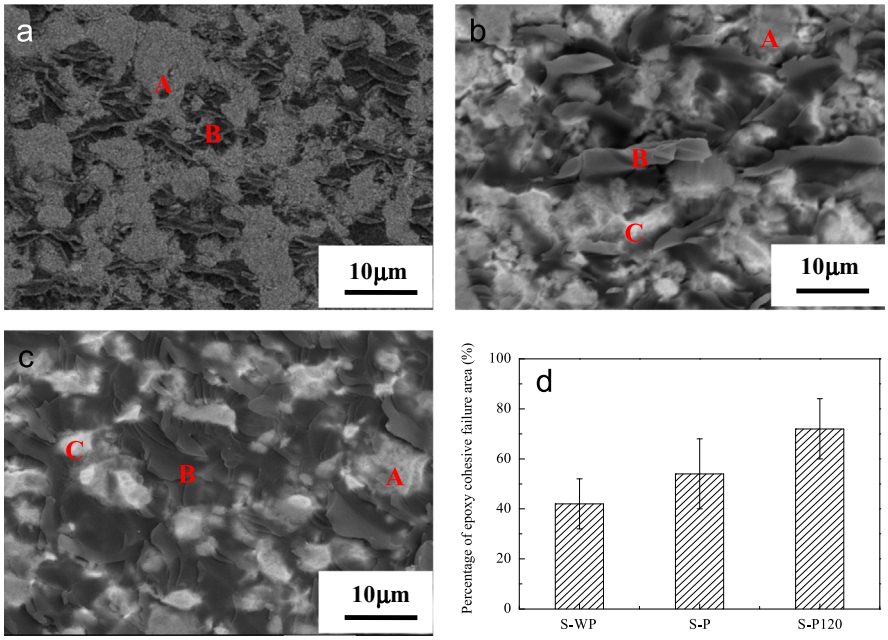

Fig. 4. Fractographs of the specimen (near to the Ti6Al4V side) after shear tests: (a) S-WP, (b) S-P, (c) S-P120, (d) percentages of epoxy cohesive failure area of each specimen. (*Notes*: "A" denotes interface adhesive failure between epoxy and anodic film, "B" denotes epoxy cohesive failure, and C denotes TiO_x failure.).

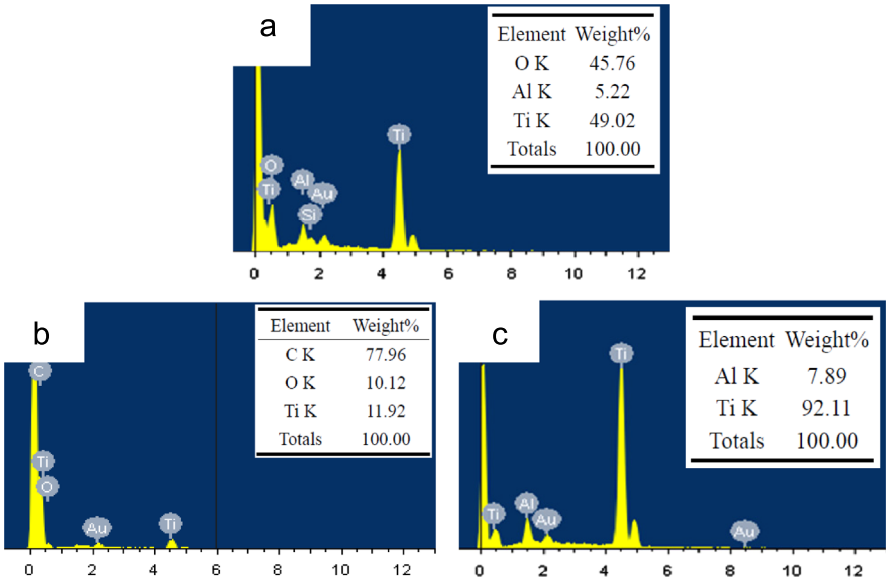

Fig. 5. EDX results from the fractograph: parts (a)–(c) corresponded to the area A–C in Fig. 3, respectively.

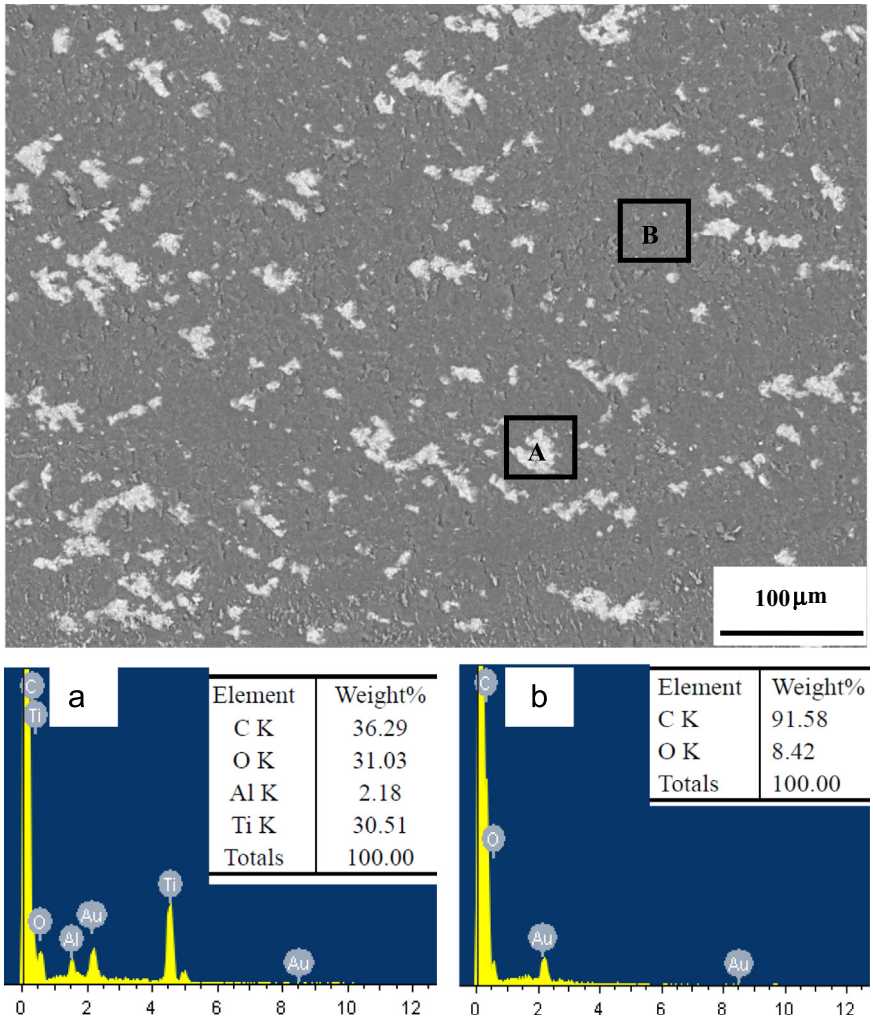

Fig. 6. Fractograph (SEM image) of the specimen S-P120 after shear tests (near to the epoxy side), and parts (a) and (b) corresponded to the EDX results of A and B areas, respectively.

Fig. 4 shows the SEM images of the fracture surface of the anodized Ti6Al4V-epoxy before and after primer application and EDX analysis, as shown in Fig. 5, to determine the failure modes. For S-WP, as discussed in our recently published paper [31], the following two failure modes occurred: (1) discontinuous cohesive failure within epoxy, which was proved by the distribution of epoxy (as indicated

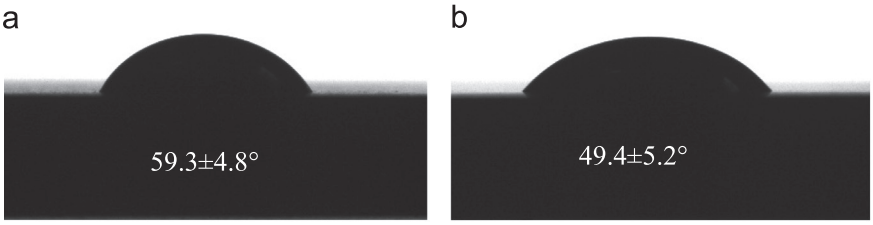

Fig. 7. Contact angle between Ti and epoxy: (a) S-P, (b) S-WP.

Table 2
Peak parameters of the standard XPS spectra of the anodized Ti6Al4V samples and primer.

Species	Binding energy (eV)	Referenced value
TiO	455.8	455.4–455.8 [43]
TiO_2	459.1	459.0–459.2 [43]
C–O	285	284.9 [44]
C–C	286.8	286.6 [44]

in the "A" area in Fig. 4(a), and they were identified by the EDX result shown in Fig. 5(a)); (2) adhesive failure between epoxy and Ti–O, which was confirmed by the emerging of anodic film (as indicated in the "B" area, and was identified by the EDX result in Fig. 5(b)). However, after application of primer, a new failure mode appeared as indicated in "C" areas in Fig. 4(b) and (c). EDX analysis, as shown in Fig. 5(c), proved only Ti and Al were detected in area C, indicating the oxide layer was peeled-off during the fracture process. Therefore, C areas corresponded to failure between anodic film-Ti substrate (TiO_x–Ti) interface or within TiO_x. Meanwhile, as shown in Fig. 6, SEM image from the epoxy side clearly confirmed the TiO_x pieces, which were peeled off from metal, were attached to the epoxy surface. Fig. 4(d) shows the percentages of epoxy cohesive failure area through image analysis in S-WP, S-P and S-P120. S-P showed a higher epoxy cohesive failure area than S-WP, and S-P120 showed the highest one. However, in Palmieri's investigation, the Ti-epoxy systems failed mainly in PETI cohesive failure rather than adhesive failure, which resulted in much higher shear strength than those in our investigation.

Based on the analysis of failure mode, it can be deduced that the increase of shear strength and different failure modes should be attributed to the following two reasons:

(1) Primer seems to increase bonding strength between epoxy and anodic film on the Ti6Al4V. This might be due to the much lower viscosity of primer (~50 mPa·s) than that of epoxy (~1000 mPa·s). For its low viscosity, wettability between primer and anodic film is much better than that of epoxy-anodic film. Fig. 7 shows the contact angle between Ti and epoxy. It proved that after the application of primer, contact angle reduced from 59.3° to 49.4°, indicating better wettability of primer to epoxy. The work of Roche proved that chemical bonding of epoxy system to Ti substrate can be formed by interfacial interdiffusion. Meanwhile, the main composition of the primer is a kind of phenolic epoxy, thus bonding strength between primer and the epoxy resin is also better than that of epoxy-anodic film. Therefore, the primer seems to act as an interface layer, which enhanced the bonding strength between epoxy-anodic film.
(2) The epoxide group content in the primer also played a key role in determining the shear strength between Ti6Al4V and epoxy. The epoxide group in the primer can react with the hardener

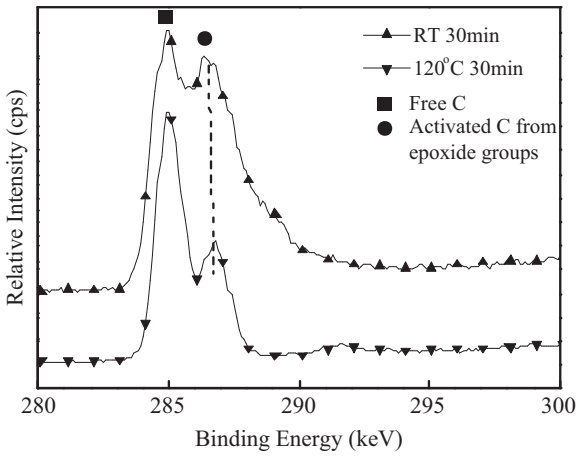

Fig. 8. XPS spectrum of primer before and after curing at 120 °C.

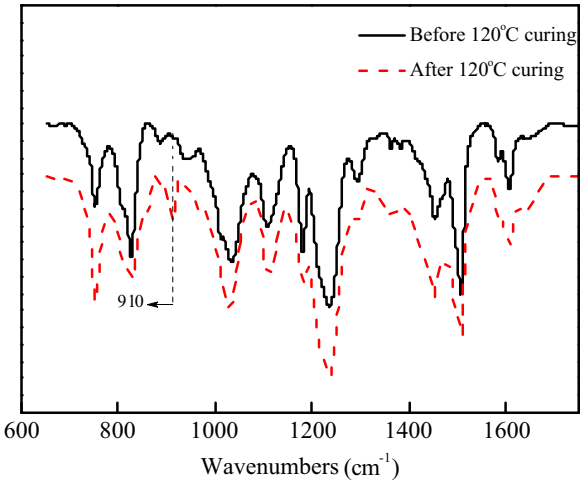

Fig. 9. IR results of pure primer before and after curing at 120 °C.

in the epoxy resin, thus increases the chemical bonding strength between primer and epoxy. Fig. 8 and Table 2 show the C XPS results of the primer before and after curing at 120 °C. After curing at 120 °C, the epoxide group content in the primer significantly decreased as compared to that without curing at 120 °C. Fig. 9 further provides the IR results from primers before and after curing at 120 °C. The intensity of peak at 910 cm^{-1} significantly reduced after 120 °C curing, which proved the decrease in epoxide group after 120 °C curing. Therefore, bonding strength between primer and epoxy in S-P120 is much higher than that in S-P, which led to higher shear strength between Ti6Al4V and epoxy.

3.2. Effects of annealing treatment of anodized Ti alloy on the shear strength

As discussed in the above, the application of primer can greatly enhance the shear strength between anodized Ti6Al4V and epoxy. However, TiO_x failure occurred within TiO_x or between TiO_x–Ti substrate, which indicated the bonding strength between anodic film and Ti substrate was poor. Xiong el al. reported that the adhesion of anodic film to Ti substrate improved greatly by annealing at 500 °C, due to changed chemistry of the interface [27]. Therefore, in our investigation, annealing was carried out in order to improve bonding strength of anodic film to the substrate. Fig. 10 and Table 2 show the Ti XPS results of the anodic film before and after annealing treatment at 500 °C in air for 5 h. For the anodic film before annealing treatment, it was composed of both TiO and TiO_2. While after annealing treatment TiO transformed into TiO_2, which played predominant role in the anodic film. So it can be deduced that after annealing treatment there was more Ti–O bonds formed in the interface between anodic film and Ti, which would lead to the improved adhesion between the anodic film and the substrate.

Fig. 11(a) and Table 3 show the shear properties of Ti6Al4V-epoxy using anodized Ti6Al4V before and after annealing treatment. It can be observed that shear strength of the specimen using anodized and annealed Ti6Al4V was 19.36 ± 0.65 MPa, which was 6.4% higher than that of specimen using only anodized Ti6Al4V, 18.20 ± 1.63 MPa. Although work of fracture showed similar increasing trends to the shear strength, it was greatly enhanced by 60.4%, from the initial 8.14 ± 0.89 kJ/m^2 to 11.44 ± 1.09 kJ/m^2. Meanwhile, fracture strain of the specimen was also increased by 63.6%, as compared with the specimen using anodized Ti6Al4V before annealing treatment.

Typical load–displacement curves from the single-lap-joint shear tests are shown in Fig. 11(b). They showed similar increasing trends but different extensions and peak loads. Both curves can be divided into two stages: (I) the initial elastic region associated with elastic deformation of the epoxy, and (II) the non-linear region associated with epoxy plastic deformation, cohesive failure and/or oxide layer failure. It was obvious that specimen using anodized and annealed Ti6Al4V showed much larger extension at break, which might be attributed to the higher epoxy cohesive failure area.

Figs. 12 and 13 present the SEM images of the detached surfaces after shear tests of specimens using anodized Ti6Al4V before and after annealing treatment. Similar to the aforementioned analysis, specimen using anodized Ti6Al4V before annealing treatment fractured in epoxy cohesive failure, epoxy-TiO_x interface adhesive failure and TiO_x failure modes, as shown in Fig. 12. However, for the specimen using anodized and annealed Ti6Al4V, TiO_x failure area decreased substantially (as shown in Fig. 13(b) and (B)), and large tracts of epoxy continuous cohesive failure occurred, as indicated in Fig. 13(a), (A) and (C). Therefore, during shear test of specimen using anodized and annealed Ti6Al4V, cracks mainly propagate within the epoxy, leading to much higher fracture strain and work of fracture than those of specimen using anodized Ti6Al4V.

It should be pointed out that failure modes of single lap joints with ductile adherends are different from that with high strength

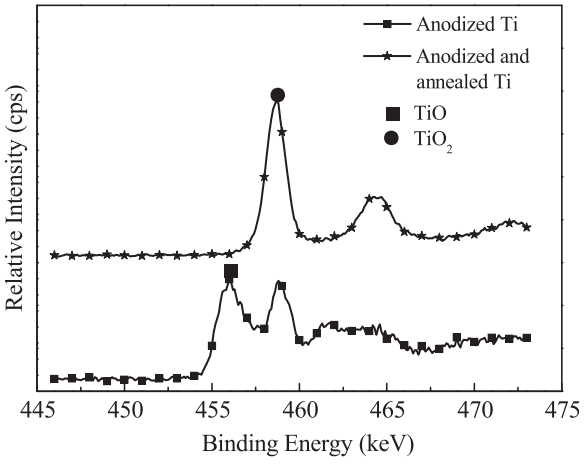

Fig. 10. XPS results of Ti element in the anodic film before and after annealing treatment.

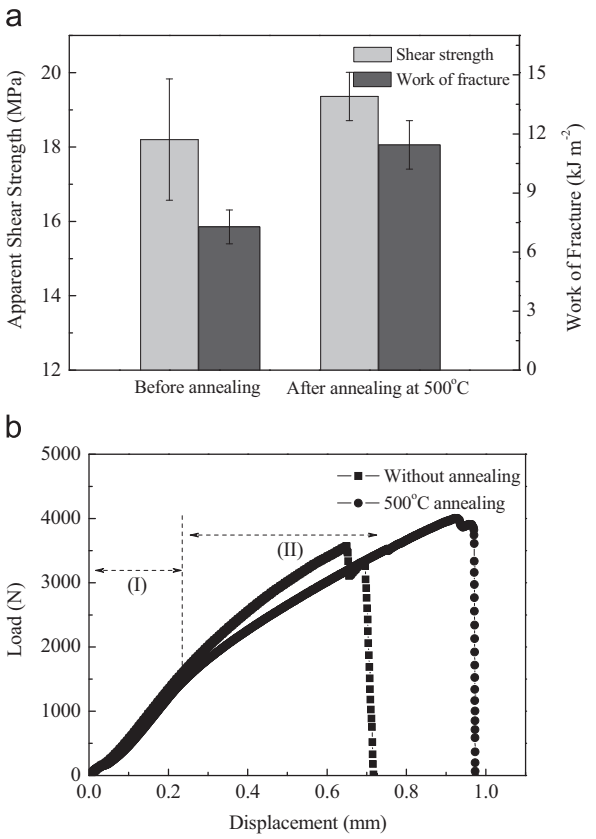

Fig. 11. (a) Shear strength and work of fracture of specimen using anodized Ti6Al4V before and after annealing treatment; (b) typical load–displacement curves of both specimens.

Table 3
Mechanical property of the specimens using anodized Ti6Al4V and the one using anodized and annealed Ti6Al4V.

Specimen	Apparent shear strength (MPa)	Work of fracture (kJ m^{-2})	Fracture strain (mm/mm)
Anodized	18.20 ± 1.63	8.14 ± 0.89	0.0275 ± 0.0050
Anodized and annealed	19.36 ± 0.65 (6.4%)	11.44 ± 1.09 (60.4%)	0.0450 ± 0.0058 (63.6%)

Note: The percentages in the brackets are the changes compared with the anodized specimens as listed in the second line in this table.

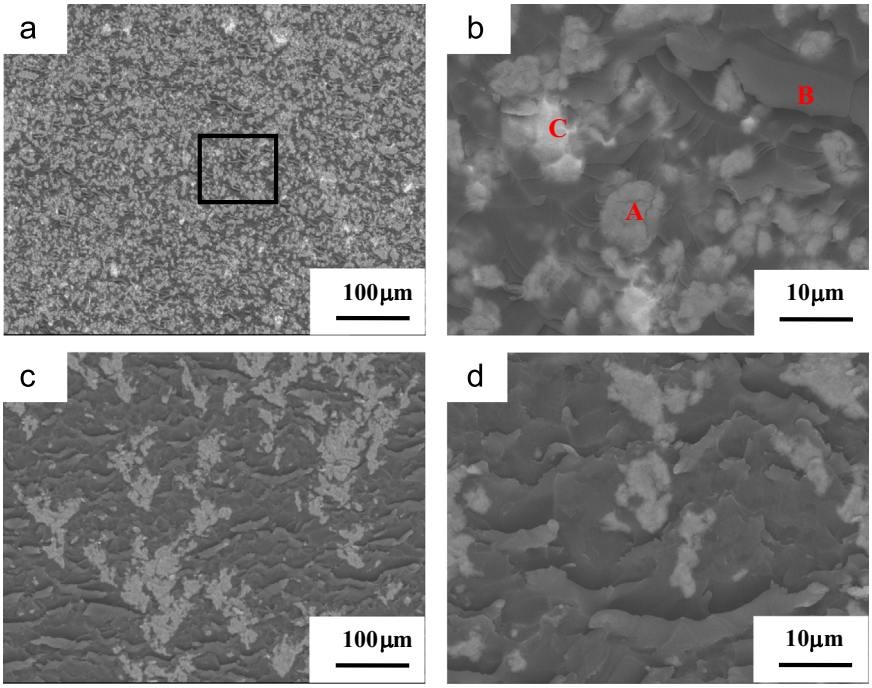

Fig. 12. Fractographs of specimens using anodized Ti6Al4V before annealing treatment: (a)–(b) Ti side, (c)–(d) epoxy side. *Notes*: "A" denotes interface adhesive failure between epoxy and anodic film, "B" denotes epoxy cohesive failure, and "C" denotes TiO_x failure.

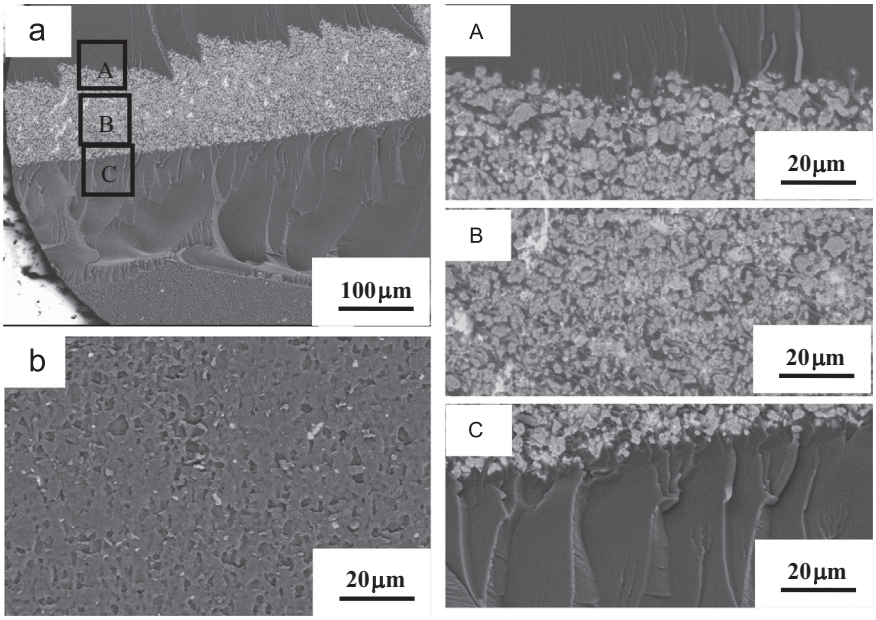

Fig. 13. Fractograph of specimens using anodized and annealed Ti6Al4V: (a) Ti side; (A)–(C) were the magnified images of areas "A"–"C"; (b) epoxy side.

adherends, as indicated in Professor Adams's researches on joints with both aluminum and high strength steel [41,42]. However, in our investigation, all the metal adherends before and after annealing presented similar yield strength (910–928 MPa), which were much higher than the hypothetically ultimate tensile strength (181.5 MPa) in our test according to Eq. (1). This indicated that during shear test only elastic deformation occurred in all the Ti adherends. Therefore, in this investigation, variation of yield strengths of both annealed and unaealed Ti adherends affected failure modes very little.

$$\sigma_t = \frac{P}{bt} \tag{1}$$

where σ_t is the hypothetical tensile strength, P is the applied load, b is the joint width, and t is the adherend thickness.

4. Conclusions

In this paper, effects of primer and annealing treatments on the shear strength between anodized Ti6Al4V and epoxy were investigated and fracture mechanisms were analyzed. The main conclusions could be drawn as below:

1. The shear strength for the specimen using anodized Ti6Al4V with primer was improved by 51.6% as compared with that of

untreated specimen. In addition, shear strength can be further enhanced by 19.6% by optimized curing strategy. Compared with the adhesive failure between epoxy–alloy interface and discontinuous cohesive failure of epoxy in the untreated specimen, anodic film failure occurred in the specimen with primer, which can be explained by the increased bonding strength between epoxy-anodic film.

2. The specimens after anodizing, annealing and primer treatment, showed the best performances in shear strength, work of fracture and extension at break by 6.7%, 60.4% and 63.6%, respectively, compared to specimen without annealing treatment. The increased mechanical properties were attributed to the large areas of continuous epoxy cohesive failure.

Acknowledgements

The authors acknowledge the financial support from the Materials Innovation for Marine and Offshore (MIMO) program with grant number of SERC1123004028 under the Agency for Science, Technology and Research (A*Star) of Singapore.

References

[1] Critchlow GW, Brewis DM. Review of surface pretreatments for titanium-alloys. Int J Adhes Adhes 1995;15:161–72.
[2] Vogelesang LB, Vlot A. Development of fibre metal laminates for advanced aerospace structures. J Mater Process Technol 2000;103:1–5.
[3] Reyes G, Cantwell WJ. The mechanical properties of fibre-metal laminates based on glass fibre reinforced polypropylene. Compos Sci Technol 2000;60:1085–94.
[4] Johnson WS, Hammond MW. Crack growth behavior of internal titanium plies of a fiber metal laminate. Composites Part A 2008;39:1705–15.
[5] Cortes P, Cantwell WJ. The prediction of tensile failure in titanium-based thermoplastic fibre-metal laminates. Compos Sci Technol 2006;66:2306–16.
[6] Coelho PG, Lemons JE. Physico/chemical characterization and in vivo evaluation of nanothickness bioceramic depositions on alumina-blasted/acid-etched Ti-6Al-4V implant surfaces. J Biomed Mater Res A 2009;90:351–61.
[7] Kim HW, Kim HE, Salih V, Knowles JC. Hydroxyapatite and titania, sol–gel composite coatings on titanium for hard tissue implants; mechanical and in vitro biological performance. J Biomed Mater Res B 2005;72:1–8.
[8] Lakstein D, Kopelovitch W, Barkay Z, Bahaa M, Hendel D, Eliaz N. Enhanced osseointegration of grit-blasted, NaOH-treated and electrochemically hydroxyapatite-coated Ti–6Al–4V implants in rabbits. Acta Biomater 2009;5:2258–69.
[9] Dagostino R, Fracassi F, Pacifico C, Capezzuto P. Plasma-etching of Ti in fluorine-containing feeds. J Appl Phys 1992;71:462–71.
[10] Man HC, Zhao NQ, Cui ZD. Surface morphology of a laser surface nitrided and etched Ti–6Al–4V alloy. Surf Coat Technol 2005;192:341–6.
[11] Allen KW, Alsalim HS. Titanium and alloy surfaces for adhesive bonding. J Adhes 1974;6:229–37.
[12] Allen KW, Alsalim HS, Wake WC. Bonding of titanium alloys. J Adhes 1974;6:153–64.
[13] Park C, Lowther SE, Smith JG, Connell JW, Hergenrother PM, St Clair TL. Polyimide–silica hybrids containing novel phenylethynyl imide silanes as coupling agents for surface-treated titanium alloy. Int J Adhes Adhes 2000;20:457–65.
[14] Yao Y, Fukazawa K, Huang N, Ishihara K. Effects of 3,4-dihydrophenyl groups in water-soluble phospholipid polymer on stable surface modification of titanium alloy. Colloids Surf, B: Biointerfaces 2011;88:215–20.
[15] Carrado A. Structural, microstructural, and residual stress investigations of plasma-sprayed hydroxyapatite on Ti–6Al–4V. ACS Appl Mater Interfaces 2010;2:561–5.
[16] Souto RM, Lemus MM, Reis RL. Electrochemical behavior of different preparations of plasma-sprayed hydroxyapatite coatings on Ti6Al4V substrate. J Biomed Mater Res A 2004;70:59–65.
[17] Roy M, Balla VK, Bandyopadhyay A, Bose S. MgO-doped tantalum coating on Ti: microstructural study and biocompatibility evaluation. ACS Appl Mater Interfaces 2012;4:577–80.
[18] Weng WJ, Baptista JL. Preparation and characterization of hydroxyapatite coatings on Ti6Al4V alloy by a sol–gel method. J Am Ceram Soc 1999;82:27–32.
[19] Yu CZ, Zhu SL, Wei DZ, Wang FH. Amorphous sol–gel SiO_2 film for protection of Ti6Al4V alloy against high temperature oxidation. Surf Coat Technol 2007;201:5967–72.
[20] Aladjem A. Review—anodic-oxidation of titanium and Its alloys. J Mater Sci 1973;8:688–704.
[21] Gemelli E, Heriberto N, Camargo A. Low voltage anodization of titanium in nitric acid solution: a new method to bioactivate titanium. Mater Charact 2011;62:938–42.
[22] He LP, Mai YW, Chen ZZ. Effects of anodization voltage on CaP/Al_2O_3–Ti nanometre biocomposites. Nanotechnology 2004;15:1465–71.
[23] Matykina E, Garcia I, de Damborenea JJ, Arenas MA. Comparative determination of TiO_2 surface free energies for adhesive bonding application. Int J Adhes Adhes 2011;31:832–9.
[24] Matz C. Optimization of the durability of structural titanium adhesive joints. Int J Adhes Adhes 1988;8:17–24.
[25] Mertens T, Gammel FJ, Kolb M, Rohr O, Kotte L, Tschocke S, et al. Investigation of surface pre-treatments for the structural bonding of titanium. Int J Adhes Adhes 2012;34:46–54.
[26] Wang J, Lin ZQ. Anodic formation of ordered TiO_2 nanotube arrays: effects of electrolyte temperature and anodization potential. J Phys Chem C 2009;113:4026–30.
[27] Xiong JY, Wang XJ, Li YC, Hodgson PD. Interfacial chemistry and adhesion between titanium dioxide nanotube layers and titanium substrates. J Phys Chem C 2011;115:4768–72.
[28] Wang YM, Jia DC, Guo LX, Lei TQ, Jiang BL. Effect of discharge pulsating on microarc oxidation coatings formed on Ti6Al4V alloy. Mater Chem Phys 2005;90:128–33.
[29] Wang YM, Lei TQ, Jiang BL, Guo LX. Growth, microstructure and mechanical properties of microarc oxidation coatings on titanium alloy in phosphate-containing solution. Appl Surf Sci 2004;233:258–67.
[30] Yang CH, Hodgson PD, Liu QC, Ye L. Geometrical effects on residual stresses in 7050-T7451 aluminum alloy rods subject to laser shock peening. J Mater Process Technol 2008;201:303–9.
[31] He PG, Chen K, Yu B, Yue CY, Yang JL. Surface microstructures and epoxy bonded shear strength of Ti6Al4V alloy anodized at various temperatures. Compos Sci Technol 2013;82:15–22.
[32] Woods GA, Haq S, Shaw SJ, Raval R. The interaction of γ-glycidoxypropyltrimethoxy silane and model analogues with the Al(1 1 1) surface. Int J Adhes Adhes 2006;26:94–102.
[33] Rider AN. Factors influencing the durability of epoxy adhesion to silane pretreated aluminium. Int J Adhes Adhes 2006;26:67–78.
[34] Abel ML, Adams ANN, Kinloch AJ, Shaw SJ, Watts JF. The effects of surface pretreatment on the cyclic-fatigue characteristics of bonded aluminium-alloy joints. Int J Adhes Adhes 2006;26:50–61.
[35] Abel M-L, Joannic R, Fayos M, Lafontaine E, Shaw SJ, Watts JF. Effect of solvent nature on the interaction of glycidoxy propyl trimethoxy silane on oxidised aluminium surface: a study by solution chemistry and surface analysis. Int J Adhes Adhes 2006;26:16–27.
[36] Abel ML, Allington RD, Digby RP, Porritt N, Shaw SJ, Watts JF. Understanding the relationship between silane application conditions, bond durability and locus of failure. Int J Adhes Adhes 2006;26:2–15.
[37] Roche AA, Bouchet J, Bentadjine S. Formation of epoxy-diamine/metal interphases. Int J Adhes Adhes 2002;22:431–41.
[38] Rider A, Chalkley P. Durability of an off-optimum cured aluminium joint. Int J Adhes Adhes 2004;24:95–106.
[39] Brack N, Rider AN. The influence of mechanical and chemical treatments on the environmental resistance of epoxy adhesive bonds to titanium. Int J Adhes Adhes 2014;48:20–7.
[40] Palmieri FL, Watson KA, Morales G, Williams T, Hicks R, Wohl CJ, et al. Laser ablative surface treatment for enhanced bonding of Ti–6Al–4V alloy. ACS Appl Mater Interfaces 2013;5:1254–61.
[41] Karachalios EF, Adams RD, da Silva LFM. Single lap joints loaded in tension with high strength steel adherends. Int J Adhes Adhes 2013;43:81–95.
[42] Karachalios EF, Adams RD, da Silva LFM. Single lap joints loaded in tension with ductile steel adherends. Int J Adhes Adhes 2013;43:96–108.
[43] Milošev I, Metikoš-Huković M, Strehblow HH. Passive film on orthopaedic TiAlV alloy formed in physiological solution investigated by X-ray photoelectron spectroscopy. Biomaterials 2000;21:2103–13.
[44] Yu B, Jiang Z, Tang X-Z, Yue CY, Yang J. Enhanced interphase between epoxy matrix and carbon fiber with carbon nanotube-modified silane coating. Compos Sci Technol 2014;99:131–40.